SS-wave reflections from conventional land 3C data

Saul E. Guevara*, and Daniel O. Trad†

ABSTRACT

This is an experiment with real data intended to identify the presence of pure S wave information (SS-waves) generated by conventional explosive sources. Currently on conventional multicomponent seismic data just PP and PS waves are usually expected and the SS wave mode is not used and even rarely identified. The Hussar 2011 3C survey data were used to this purpose. From modeling using the available velocity information, SS-waves arrive inside the Ground Roll cone. Therefore it is required noise attenuation of events such as surface waves preserving as much as possible the expected SS-waves. The resulting records show energy with the expected SS arrival time in both radial and transversal components, even though easier to identify in the transversal component. Experiment for S-wave source static corrections, together with a velocity analysis, allowed to obtain SS stack sections, both for the transversal and radial components. Interestingly, even though the analysis were carried out on the transversal component, the radial component shows a better signal. Some events can be identified at the expected arrival time. The method appears promising to obtain additional information of 3C data.

INTRODUCTION

In conventional seismic surveys just PP and PS waves are usually expected and SS reflections have been hardly identified. However S-wave generation has been predicted for theoretical models of real energy sources, such as elastic waves generated at the free surface (e.g. Miller and Pursey, 1954) and explosive sources inside boreholes (e.g. Lee and Balch, 1982). Experiments that confirm these models have been also published (e.g. Hardage and Wagner, 2014; Lash, 1985). This work presents an efford that intends to identify the presence of pure S-wave reflections (SS-waves) in real conventional multicomponent data, and to explore methods for its initial processing. We use to this purpose the data of a multicomponent experimental survey acquired by the CREWES project, the Hussar 2011 3C.

Firstly it was estimated the SS waves arrival time and NMO curve from the velocity model of the zone, which was compared to the field records, taking into account the elusive nature of these events. After that strategies to enhance the possible SS-waves are investigated, as much as the statics correction for the source generated S-wave. Finally a velocity analysis was carried out which allowed to obtain and analise stacked sections.

THEORY

A number of theoretical works show that S-waves are generated by energy sources on the ground surface (e.g. Miller and Pursey, 1954) or inside a borehole (e.g. Lee and Balch,

*Santander Industrial University
†CREWES / Univ. of Calgary

1982), usual in onshore seismic exploration. Hence we would expect the presence of SS-reflections (generated as S and reflected as S) from the geological interfaces recorded at the surface. Velocity of S-waves is about half the P-wave, hence their arrival time would be about twice. However the reflection is symmetrical, therefore some of the PP processing hypothesis are also valid, such as the Common Mid Point model (Yilmaz, 2001). An useful approximation to the hyperbolic NMO curve, including the stacking (or NMO) velocity, is given by the Dix Equation (Yilmaz, 2001). For SS waves at the k_{th} layer this velocity reads

$$\left(V^k_{SS_{rms}}\right)^2 = \frac{\sum_{i=1}^{k}(V^i_S)^2\,(2\Delta t^i_S)}{\sum_{i=1}^{k} 2\Delta t^i_S} \tag{1}$$

where Δt^i_P is the one way zero offset traveltime spent by the S-wave through layer i, and V^i_S is the interval velocity at the i layer. Traveltime is calculated according to

$$\Delta t^i_S = \frac{\Delta z_i}{V^i_S}, \tag{2}$$

where Δz_i is the layer thickness, and the arrival time is

$$t^k_{SS} = \sum_{i=1}^{k} \Delta t^i_S. \tag{3}$$

Ground Roll is composed by surface (or Rayleigh) waves, which are typically linear, low frequency, usually dispersive, with an estimated velocity of about 97% the S-wave, and posses about 60% of the total energy. Other events, such as S-wave refractions, are also possibly inside the GR. Therefore filtering methods that take into account their difference with the SS-wave reflections are required, some of them in the frequency wave-number domain.

The static corrections aim to overcome the delay caused by the near surface layer (NSL) on seismic waves reflected at deeper layers. Since S-waves propagate more slowly and are not affected by the water table, the NSL effect is more severe on this type of data. Hence we can expect more challenging static corrections for SS reflections since they travel twice (source and receiver sides) through the NSL (Anno, 1986). The assumption behind static corrections is the surface consistency, namely that all the traces arriving to the same receiver or departing from the same source have the same NSL delay (Cox, 1999). This is a robust and practically proved model. It is expressed by the surface consistent equation (e.g. Schneider, 1971; Yilmaz, 2001), which is presented by Taner et al. (1974) as:

$$T_{ijk} = R_i + S_j + G_k + M_k h^2_{ij} \tag{4}$$

where R_i denotes receiver statics at the i_th receiver position. S_j denotes Source statics at j_th source position. G_k denotes an arbitrary time shift for kth CDP gather, also known as *structural geology* component (or normal incidence time). M_k denotes residual NMO component at kth CDP gather, and h_{ij} denotes source to receiver distance [‡]. The CDP corresponds to the index k, the CSG to the index j and the CRG to the index i.

[‡]Taner et al. (1974) use $(j-i)$ instead

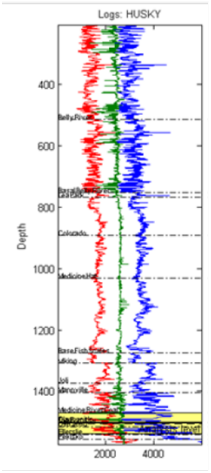

a

Depth m	Vp m/s	Vs m/s	t_o PP s	V_{PP} RMS m/s	t_o PS s	V_{PS} RMS m/s	t_o SS s	V_{SS} RMS m/s
30	1500	200	0.040	1500	0.170	548	0.300	200
400	2900	1500	0.291	2844	0.599	1640	0.907	1207
520	3400	1100	0.362	3094	0.743	1701	1.125	1168
750	3300	1500	0.503	3179	0.960	1845	1.416	1399
1270	3250	1500	0.803	3392	1.472	2060	2.013	1645
1450	3900	1900	0.901	3454	1.623	2111	2.217	1664
1550	4400	2200	0.949	3585	1.694	2155	2.310	1745

b

FIG. 1. The velocity information obtained from the sonic logs. (a) The sonic log including the P-wave velocity (blue), and the S-wave velocity (red). (b) Table of the RMS (approx. stacking) velocities and zero offset (t_0) arrival times for PP, PS, and SS-waves. The depths and estimated P-wave and S-wave velocities are in the first three columns.

DATA ANALYSIS

The seismic line selected is 4.5 Km length, and comprises 257 shot records, whose sources are nominally 20 m appart, and recorded by 448 multicomponent receivers, separated 10 m to each other. Source energy is provided by dynamite buried in boreholes at 15 m depth. The topography is mostly flat, with a 70 m high and about 2% slope to the NW. More information about the Hussar 2011 survey is in CREWES reports, such as Margrave et al. (2011).

Figure 1(a) illustrates the sonic logs for P-and S-wave at the Hussar line. From these data, a blocked model was created and the RMS velocities were calculated using the Dix Equation. The resulting zero-offset arrival times and RMS velocities for PP, PS and SS waves are shown in the Table of Figure 1(b).

Raw data analysis and filtering

Two raw records of the radial and transversal components of the same shot are illustrated in Figure 2. From the velocity and depth information of Table 1(b) it is possible to calculate the arrival times of the SS-reflections, and the estimated expected arrival times of two highlighted events (yellow color in the Table of Figure 1(b)) are shown as red lines in Figure 2. It can be noticed the strong Ground roll cone in both components, usually identified as coherent noise, and that the NMO curves corresponding to the estimated arrival time of the two SS reflections are totally embedded in the GR cone.

As a consequence, to obtain information of the SS-reflections it is required filtering or attenuation of the other GR events such as surface waves, preserving as much as possible the expected SS-waves. This is a challenging endeavour taking into account the strong energy usually shown by surface waves and the possibly weak signal of the SS reflec-

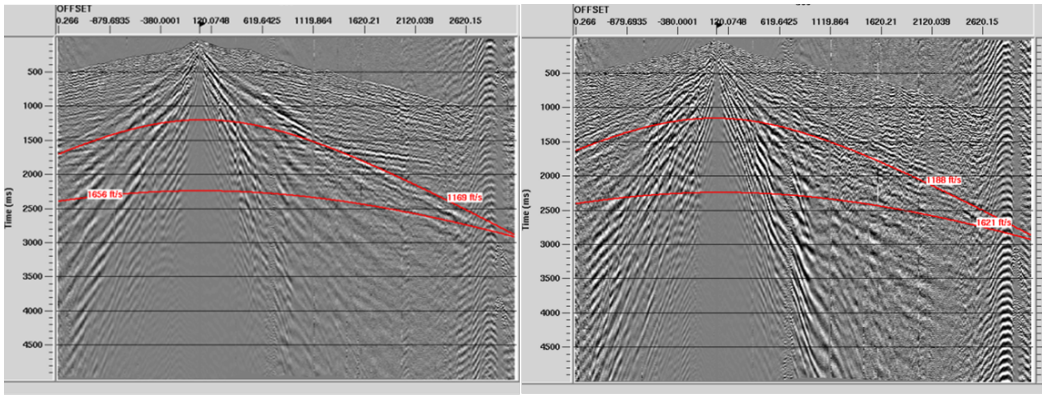

FIG. 2. Comparison of the radial and transversal components of a shot without filtering.

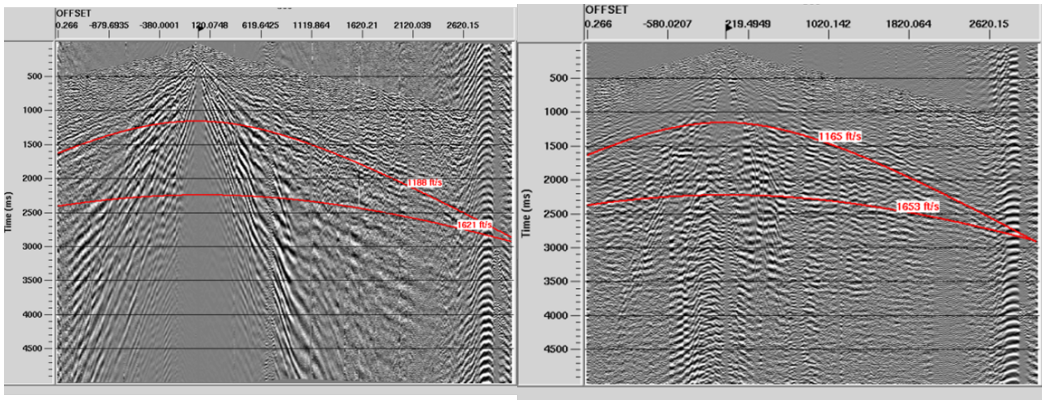

FIG. 3. Comparison of a shot before filtering and after filtering.

tions. Processes useful to this purpose in ProMAX include surface wave noise attenuation, noise burst edition and bandpass filtering. In addition it appeared useful applying the Time Fourier Transform filter.

Figure 3 shows the transversal component before (Fig. 3a) and after (Fig. 3b) filtering. Notice that many linear events have been attenuated, and some events that follows the NMO curves (analogous to the curves of Fig. 2) can be identified. Figure 4 shows both component records after filtering, the radial component in Fig. 4a and the transversal in Fig. 4b. Notice that the events identified as SS-waves appear easier to follow in the transversal component and in the radial component are harder to follow and a strong coherent event appears, which we can identify as converted waves (PS) by its arrival time and NMO curve. As a consequence, we selected the transversal component for the next analyses.

Static corrections experiment

Two families of static corrections approaches can be identified: methods that require a velocity model of the NSL, and methods that take advantage of the crosscorrelations to obtain the time delay (Cox, 1999).

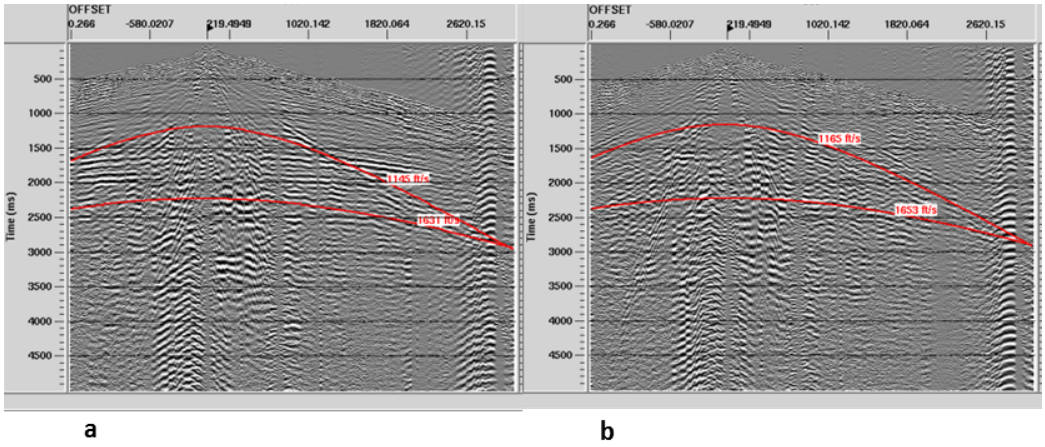

FIG. 4. Comparison of the radial and transversal components of a shot after filtering.

Static corrections for S-waves are more difficult obtaining compared to P-waves, since methods to obtain the NSL S-wave velocity are less reliable, and probably overlook short wavelength effects. In addition, there is not uphole time information for S-wave, a piece required in the source statics calculation. On the other hand, there are proved methods to obtain the receiver component statics of PS-waves by crosscorrelation, assuming a previous P-wave source statics solution obtained from the PP-wave processing (Harrison, 1992). The Hussar's PS seismic section obtained by CREWES exhibits such a robust solution (see Fig. 8b), therefore we can assume that the receiver statics of SS events is already solved, and just require a method for the source S-wave statics.

Taking into account the previous analysis we propose a method following the approach in Guevara and Margrave (2014), that is obtaining the near surface differential delay between adjacent gathers by cross-correlation between analogous traces of them, and taking advantage of the surface consistent equation (Eq. 4), however using differential time delays instead, symbolized by δ. This equation reads

$$\delta T_{ijk} = \delta R_i + \delta S_j + \delta G_k + \delta N_{ijk} \tag{5}$$

where δR_i denotes the differential receiver statics at the receiver position i_{th}. δS_j denotes the differential source statics at the source position j_{th}, and δG_k denotes the differential geological structure time shift for the kth reflection gather. δN_{ijk} denotes the differential NMO effect at the kth reflection gather with source j and receiver i.

If we have already solved the receiver statics, offset is the same on both traces, and assume a negligible geological structure component, the differential delay would be equal to the source S wave statics. This differential delay can be found by cross-correlation. The resulting cross-correlation of all the sources is shown in Fig. 5a, and the corresponding picks are shown in Fig. 5b. According to the model stated, these picks correspond to the differential statics between sources, therefore the static corrections with respect to a datum can be obtained by the cumulative summation of them. Unfortunately it was not as successful in our source experiment, since it appears a bias toward the high source number (Fig. 5c). Numerically it was estimated a bias effect and subtracted from the static corrections previously obtained, resulting a new solution shown in Fig. 5d. After applying the last

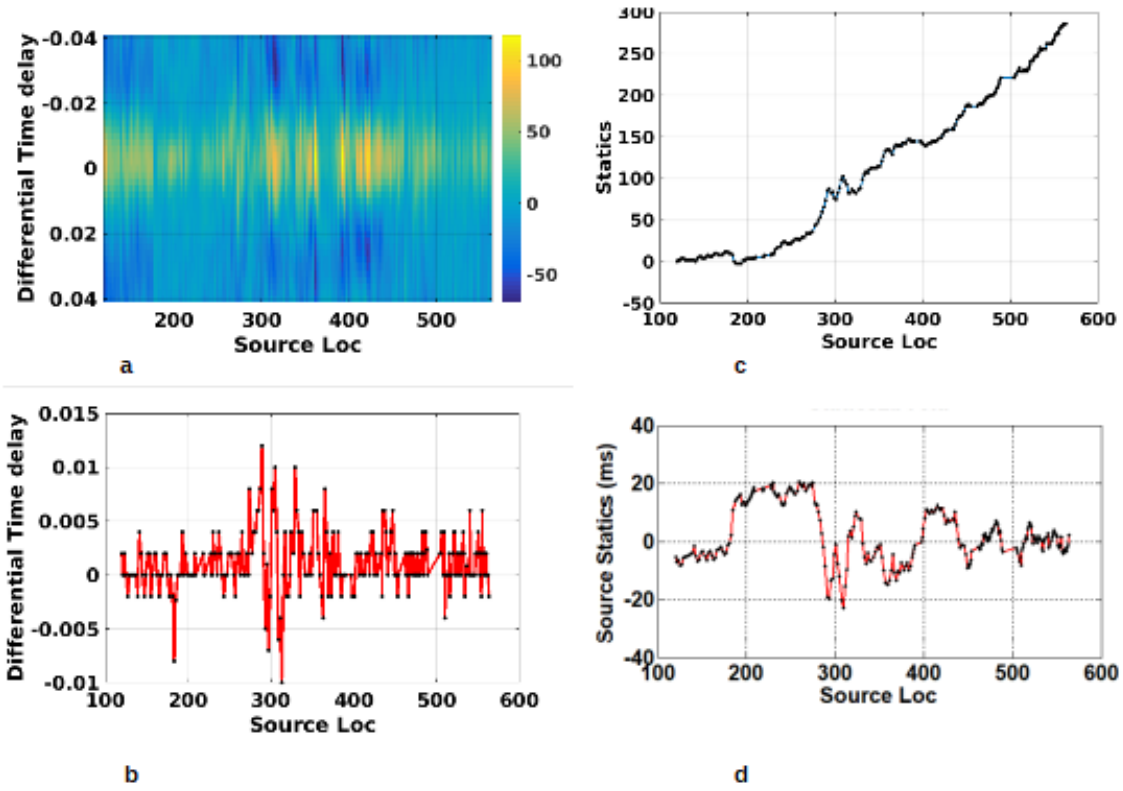

FIG. 5. Test of the source static corrections method using crosscorrelations between analogous traces of adjacent shots. (a) Resulting crosscorrelations along all the shots; (b) Picking of the maximum crosscorrelation energy, which in principle should correspond to the differential delay; (c) Static corrections from adding the differential delays; (d) Static corrections after subtracting a bias effect.

result is was obtained a better image. More on the statics is analyzed in the next section.

Static corrections, velocity analysis and stacking

Another approximation to the source statics can be obtained from the interpolation of the receiver statics used for the PS wave, since it corresponds also to an S wave traveling through the NSL. This statics solution is shown in Fig. 6a, by the continuous blue line. As for comparison, the result of the previous experiment, shown in Fig. 5d), is also displayed in this figure as a red dashed line. Notice some correlation between both statics solutions. However, after comparing stacked sections, the interpolated static corrections (blue line in Fig. 6) yields a better image, hence it was selected for the following steps.

After filtering and the source and receiver static corrections applied, a conventional velocity analysis was carried out. The resulting velocity model is shown in Fig. 6b, which can be compared to the RMS velocity data of the Table in Fig. 1b to check its reliability.

Using the previous results, it was possible to obtain stacked sections for the transversal and radial components after the NMO correction, which are shown in Fig. 7, the transversal component in Fig. 7a and the radial in Fig. 7b. Notice that the radial component section appears more coherent, which is someway surprising, taking into account that the analyses

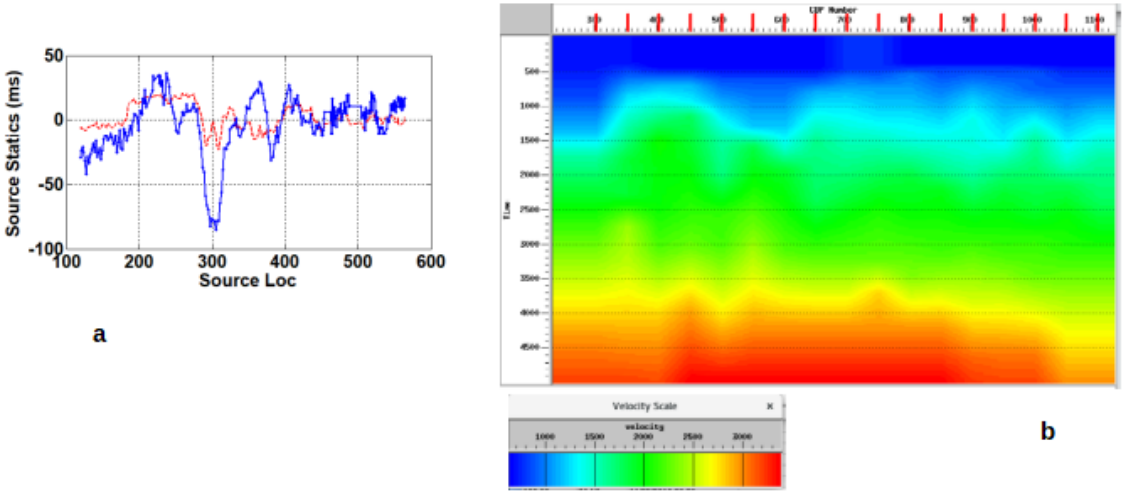

FIG. 6. Stack section parameters. (a) Source static corrections obtained from interpolation of the receiver statics (blue line); as for comparison, a result of the previous experiment (Fig. 5d) is shown as a red dashed line; (b) stacking SS velocity from the velocity analysis.

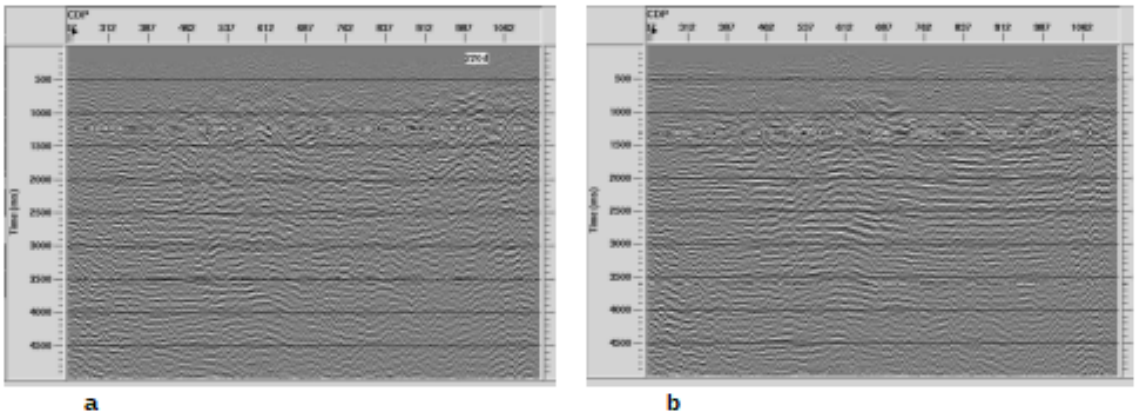

FIG. 7. Comparison of SS stack sections of the (a) transversal and (b) radial components.

were carried out mostly on the transversal component.

Fig. 8 shows a comparison of the two stacked sections, the SS radial component with the PS section obtained by a previous processing in the CREWES project (Isaac and Bancroft, 2012). Both figures have the same vertical and horizontal scales (time and CDP surface location). The red arrows show probable analogous events in both sections, coming from the same geological interface. See Table in Fig. 1b as a reference for this comparison.

Notice that there is an anomalous time shift in the SS events at about CDP 600, compared to the PS section. Surface elevations for the CDPs are shown by the line above in Fig. 8a. The anomalous time shift make sense assuming correct SS reflections and a source statics unsolved issue, related to the topography. since there is a correlation between the elevation high at about CDP 600 and this anomalous time shift.

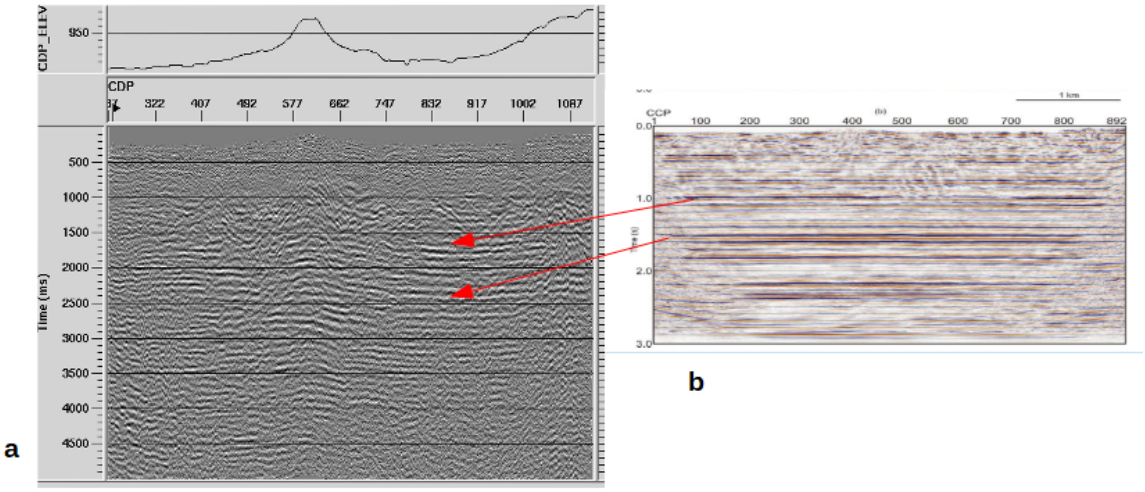

FIG. 8. Comparison of the events of the (a) SS stack section from the radial component and (b) the PS stack section. Both have the same time and space scales. The red arrows identifies analogous events.

DISCUSSION

The stacked section of Fig. 8a shows reliable SS reflection events, since they appear at the expected arrival time and with NMO velocities that also agree with the expectations for these wave type (Fig. 6b and Table 1b), besides the presence of strong coherent noise in the radial component (Fig. 4a). In addition, these events can be related to events identified in the PS section (Fig. 8).

Although the main purpose of this work, that is to say, to identify SS reflections in conventional multicomponent land data, seems to be fulfilled, there are a number of issues that demand attention, looking for application of these SS events to practical problems. Thus, the source statics correction and the surface waves noise attenuation appear as major challenges.

The datum statics methods require a S-wave NSL velocity model, which is not easy to obtain reliably and with the required detail. Refraction methods lacks of reliable events to pick, and surface wave methods appear missing local details (e.g. AlDulaijan, 2008; Schafer, 1993). On the other hand, the NSL S-wave velocity model (see Guevara et al., 2013) present issues to take into account. As an example, the shallower near surface (less than about 15 m depth in Guevara, 2017) appears as the most influential, since its velocity can be less than 200 m/s, consequently the S-wave time delay can be quite significant, and it is not easy to obtain such a low velocity data (Guevara, 2017). In addition explosive sources are buried some meters inside the ground, therefore there is an additional delay.

Therefore methods for statics corrections that take advantage of the reflections delay appear advisable. That is the rationale of experimental static corrections method proposed. An analogous approach allowed reliable results for the PS receiver statics (see Guevara and Margrave, 2014; Guevara, 2017). The results in this case do not appear encouraging. However it does not appear totally erroneous, as shown by Fig. 6a. A key problem appears

to be the low strength of the S reflections signal, as shown in Fig. 4. Therefore better signal filtering should contribute to improve this static corrections method. Other steps such as trace interpolation and crosscorrelation, as much as the time delay caused by the geological structure also deserve attention.

By the way, measurement of the S wave shot uphole time using multicomponent receivers at the ground level can be quite useful. In fact, if the S-wave velocity were 200 m/s and the borehole depth 15 m (like in Hussar), there were a meaningful 45 ms delay to the surface. This delay is a source of error in the interpolation of receiver statics.

High-energy coherent-noise filtering methods also deserve attention, focused in keeping the simultaneous low energy SS reflections, which is not the focus of currently used methods. Research on this topic can be quite profitable to obtain a better image with SS.waves.

SUMMARY AND CONCLUSIONS

1. Modeling of the NMO SS curves based on sonic well logs allowed to conclude that the feasible SS-waves coincide with the ground roll cone.

2. Noise attenuation focused on the ground roll, to attenuate surface waves preserving the hypothetical SS reflections was carried out, and the shots gathers, after noise attenuation, show events whose energy agree with the expected arrival time of SS waves.

3. These events are easier to identify in the transversal component, hence the next analyses were carried out on this component.

4. Source static corrections are a major challenge for these data. An experimental statics method, based on corosscorrelation of traces of adjacent shot gather after receiver statics, was proposed. The result shows a noticeable bias. However we propose that more research on this methods can be rewarding

5. After source statics obtained from extrapolation of the receiver statics and a velocity analysis, the SS-wave stacked section of the radial component, shows events that correlate nicely with the PS-wave stacked section.

6. The result is promising for a new technology of SS-wave applications in seismic exploration.

7. There is room for research in noise attenuation and S-wave source statics correction.

8. It is proposed S-wave uphole time recording during the acquisition stage of multicomponent. This datum can contribute noticeably to the S-wave source statics correction,

ACKNOWLEDGEMENTS

We thank the sponsors of CREWES who supported this research. We also gratefully acknowledge support from NSERC (Natural Science and Engineering Research Council of

Canada). CREWES staff contributed greatly. Special recognition to Kevin Hall and Kevin Bertram for their computing and operational support. Useful suggestions were provided by Helen Isaac and Jose Fernando Gamboa. We would also like to thank Halliburton for the use of donated SeisSpace software.

REFERENCES

AlDulaijan, K., 2008, Near-surface characterization using seismic refraction and surface-wave methods: M.Sc. thesis, Univ. of Calgary.

Anno, P. D., 1986, Two critical aspects of shear wave analysis: statics solutions and reflection correlations, *in* Danbom, S. H., and Domenico, S. N., Eds., Shear-wave exploration, Society of Exploration Geophysicists: Geophysical Developments Series, 48–61.

Cary, P. W., and Eaton, D. W., 1992, A simple method for resolving large converted-wave P-SV statics: Geophysics, **58**, No. 3, 429–433.

Cox, M., 1999, Static corrections of seismic reflection surveys: SEG Geophysical Reference Series, Tulsa, OK, USA.

Guevara, S. E., 2017, PS-wave processing in complex land settings: statics correction, wave-mode separation, and migration: Ph.D. thesis, Univ. of Calgary.

Guevara, S. E., and Margrave, G. F., 2014, Receiver statics correction of ps-wave using pre-stack data in the receiver domain: CREWES Research Report, **26**, 27.1–27.15.

Guevara, S. E., Margrave, G. F., and Agudelo, W. M., 2013, Near surface S–wave velocity from an uphole experiment using explosive sources: 83th Ann. Internat. Mtg., Soc. Expl. Geophys. Expanded Abstracts, 1694–1698.

Hardage, B. A., and Wagner, D., 2014, Generating direct-S modes with simple, low-cost, widely available seismic sources: Interpretation, **2**, SE1–SE15.

Harrison, M. P., 1992, Processing of PSV surface-seismic data: anisotropy analysis, dip moveout and migration: Ph.D. thesis, Univ. of Calgary.

Isaac, J. H., and Bancroft, J. C., 2012, Hussar converted-wave data processing and analysis, *in* CREWES Research Report, vol. 24, 44.1–44.12.

Lash, C. C., 1985, Shear waves produced by explosive sources: Geophysics, **50**, 1399–1409.

Lee, M. W., and Balch, A. H., 1982, Theoretical seismic wave radiation from a fluid-filled borehole: Geophysics, **47**, 1308–1314.

Margrave, G. F., Mewhort, L., Phillips, T., Hall, M., Bertram, M. B., Lawton, D. C., Innanen, K., Hall, K. W., and Bertram, K., 2011, The Hussar low-frequency experiment, *in* CREWES Research Report, vol. 23, 78.1–78.24.

Miller, G. F., and Pursey, H., 1954, The field and radiation impedance of mechanical radiators on the free surface of a semi-infinite isotropic solid: Proceedings of the Royal Society of London. Series A, Mathematical and Physical Sciences, **223**, 521–541.

Schafer, A. W., 1993, Binning, static correction, and interpretation of P-SV surface-seismic data: M.Sc. thesis, Univ. of Calgary.

Schneider, W. A., 1971, Developments in seismic data processing and analysis (1968-1970): Geophysics, **36**, 1043–1073.

Taner, M. T., Koehler, F., and Alhilali, K. A., 1974, Estimation and correction of near-surface time anomalies: Geophysics, **39**, No. 4, 441–463.

Yilmaz, O., 2001, Seismic data analysis: processing, inversion and interpretation of seismic data: Society of Exploration Geophysics, Investigations in Geophysics No. 10.